Advances in Computational Mathematics (2026) 52:10
https://doi.org/10.1007/s10444-026-10281-z

A comparative numerical study of spectral properties in isogeometric collocation and Galerkin methods for acoustic waves

Elena Zampieri[1]

Received: 14 April 2025 / Accepted: 7 January 2026

Abstract
We approximate the acoustic wave equation in two-dimensional regions using collocation and Galerkin isogeometric analysis (IGA) in space, coupled with implicit second-order Newmark schemes for time integration. We present a detailed numerical study that examines and compares the behavior of extreme eigenvalues and condition numbers of the mass and iteration IGA matrices, varying the polynomial degree p, mesh size h, regularity k, and the boundary conditions, that can be either Dirichlet or absorbing in order to simulate unbounded domains. We propose and validate numerically some conjectures related to the IGA collocation and Galerkin matrices for the wave equation with different types of boundary conditions, extending similar results that are known for the IGA Galerkin approximation, limitedly to the case of the Poisson problem with Dirichlet boundary conditions, and generalizing earlier results obtained within the framework of the collocation method. The results show that the spectral properties of the IGA collocation matrices are analogous and in most cases better than the corresponding IGA Galerkin discretization of the Poisson problem with Dirichlet or absorbing boundary conditions.

Keywords Acoustic waves · Isogeometric analysis · Collocation · Galerkin · Condition number

Mathematics Subject Classification (2010) 65M06 · 65M70 · 65M12

Communicated by: Lourenco Beirao da Veiga

E. Zampieri has been supported by grants of MIUR (PRIN 202232A8AN_003 and PRIN P2022B38NR_002), funded by European Union - Next Generation EU, and by grants of the Istituto Nazionale di Alta Matematica (INdAM - GNCS), Italy.

✉ Elena Zampieri
elena.zampieri@unimi.it

[1] Department of Mathematics, Università di Milano, Via Saldini 50, 20133 Milano, Italy

1 Introduction

Isogeometric analysis (IGA) has been successfully applied across a wide range of fields since its introduction in [20], yielding significant results in various practical problems involving the numerical solution of partial differential equations (PDEs) (see, e.g., [1, 6, 7, 9], and the references therein). Within the IGA framework, recent studies have focused on explicit acoustic and elastic wave problems, employing Galerkin, discontinuous Galerkin, and collocation methods (see, e.g., [3, 10, 15, 21, 23, 36–38]). IGA methods are based on the use of the same functions to both construct the CAD geometry and represent the approximate solution of the PDEs. This approach ensures an exact representation of the computational domain while also achieving higher-order approximation accuracy compared to standard p- and hp- refinements, where p denotes the polynomial degree of the IGA basis functions and h refers to the mesh size of the elements. IGA also allows for an additional k-refinement, where $k \leq p-1$ represents the global regularity of the IGA basis functions. While early IGA studies focused on Galerkin approaches, more recent research has increasingly explored IGA collocation methods. The latter methods aim to produce sparser mass and stiffness matrices compared to their IGA Galerkin counterparts. Additionally, IGA collocation offers the advantage of reducing the overall computational cost, as collocation matrices require only one function evaluation per collocation point, regardless of the polynomial degree p (see [3, 15, 23]).

In our previous works [36]-[38], we have studied and compared the stability and convergence properties of Galerkin and collocation IGA approximations for the acoustic wave equation with Dirichlet, Neumann, and absorbing boundary conditions, using Newmark's schemes for time integration. Specifically, to simulate unbounded domains, we have focused on absorbing boundary conditions that involve only first-order derivatives in both space and time (see, e.g., [4, 5, 8, 14, 18, 26] and the review paper [33]). Alternative approaches to address outgoing radiation problems include the use of absorbing boundary conditions with higher-order derivatives in both space and time, as well as employing perfectly matched layer (PML) boundary conditions (see [4, 5, 33, 35]).

Since neither the IGA collocation nor the Galerkin mass matrices are diagonal, solving the linear systems at each time step becomes a critical aspect for both explicit and implicit Newmark schemes. Unfortunately, there is a lack of theoretical results in the literature regarding IGA matrices, particularly for IGA collocation. Most of the existing estimates on the conditioning of the IGA mass and stiffness matrices remain conjectural. For instance, in [16, 17, 19], they provide results for IGA Galerkin matrices associated with the Poisson problem and Dirichlet boundary conditions. In the absence of theoretical bounds on the condition number of the IGA mass and stiffness matrices—especially for wave problems—we conducted an extensive numerical investigation of the spectral properties of IGA matrices in the collocation framework, as detailed in [39].

The main new contribution of this paper is a comprehensive numerical investigation of the spectral properties of IGA Galerkin mass and iteration matrices for the acoustic wave equation with Dirichlet or absorbing boundary conditions. We also provide a direct and thorough numerical comparison between the collocation and Galerkin IGA

methods, employing Newmark schemes for time integration. Specifically, we study and compare the behavior of their extreme eigenvalues and condition number, while varying key parameters of the spatial discretization, such as polynomial degree p, mesh size h, regularity k, and of the temporal discretization, such as time step Δt and Newmark parameter β. We deduce some conjectures about their dependence on the discretization parameters, generalizing and improving previous results obtained in [19] for IGA Galerkin in the case of Poisson problem and in [39] in the case of wave equations. Furthermore, we examine the case of heterogeneous acoustic wave propagation velocity within the computational domain, modeled either by a smooth function or a piecewise-constant function.

Our numerical results demonstrate that the condition numbers of the IGA collocation and Galerkin mass and stiffness matrices exhibit similar trends with respect to the mesh size h, and these findings are consistent with those reported in [16, 19] for the Poisson problem. When examining the behavior of the condition number as the polynomial degree p increases, we observe that the condition number is generally more favorable for IGA collocation than for IGA Galerkin, regardless of whether the regularity k is minimal or maximal.

These results are not only relevant to acoustic wave equations but also to a wide range of PDEs that trace back to the Laplacian operator. They also provide an important starting point for developing efficient preconditioning methods for iteration matrices, applicable to both explicit and implicit time-stepping schemes [40].

The rest of the paper is organized as follows: The acoustic wave model problem is introduced in Section 2. In Section 3, we describe its approximation by IGA collocation and Galerkin in space and by Newmark scheme in time. In Section 4, after a brief overview of the existing literature for eigenvalue and condition number estimates of IGA Galerkin approximation of the Poisson problem, we propose some additional conjectures that we assume to apply for IGA collocation or Galerkin approximations of the acoustic wave equation with Dirichlet and absorbing boundary conditions. Finally, in Section 5, we present several numerical tests, varying all the discretization parameters.

2 The acoustic wave model problem

Let Ω be a finite region in the plane, $\partial\Omega$ is its boundary, and $\mathbf{n}$ is the outward normal unit vector. We consider the acoustic wave problem (see, e.g., [22]):

$$\frac{\partial^2 u}{\partial t^2}(\mathbf{x}, t) - c_0 \Delta u = f(\mathbf{x}, t) \quad \text{in } \Omega \times (0, T), \tag{1}$$

with initial conditions

$$u(\mathbf{x}, 0) = \mathcal{U}_0(\mathbf{x}), \qquad \frac{\partial u}{\partial t}(\mathbf{x}, 0) = \mathcal{W}_0(\mathbf{x}) \qquad \text{in } \Omega. \tag{2}$$

The boundary conditions can be standard Dirichlet or Neumann

$$u(\mathbf{x},t)=\Phi(\mathbf{x},t)\quad \text{on } \Gamma_D\times(0,T),\qquad \frac{\partial u}{\partial \mathbf{n}}(\mathbf{x},t)=\Psi(\mathbf{x},t)\quad \text{on } \Gamma_{Ne}\times(0,T). \tag{3}$$

On the other hand, since wave propagation problems are usually set in unbounded domains, one of the most common strategy in order to refer to a finite domain Ω in (1) is to enforce absorbing boundary conditions (ABCs for brevity) rather than standard Dirichlet or Neumann ones, with the aim of truncating the original unbounded domain into a finite one, thus reducing spurious wave reflections as far as possible. In this regard, we consider here natural ABCs involving first spatial and temporal partial derivatives only (see, e.g., [4, 5, 8, 14, 18, 26] and the review paper [33]):

$$\frac{1}{\sqrt{c_0}}\frac{\partial u}{\partial t}(\mathbf{x},t)+\frac{\partial u}{\partial \mathbf{n}}(\mathbf{x},t)=0\qquad \text{on } \Gamma_{AB}\times(0,T), \tag{4}$$

where Γ_{AB} is the artificial boundary, where ABCs are enforced, $\partial\Omega\equiv\Gamma=\Gamma_D\cup\Gamma_{Ne}\cup\Gamma_{AB}$ is the boundary, and Γ_D, Γ_{Ne} and Γ_{AB} are disjoint sets.

In the above equations, c_0 is the acoustic wave propagation velocity, f is the source term, $\mathcal{U}_0$ and $\mathcal{W}_0$ are the initial pressure and velocity, respectively, u is the unknown pressure, $\mathbf{x}$ is any point of Ω, t is the time variable, and $(0,T)$ is the temporal interval, with $T\in\mathbb{R}^+$.

We make the assumption that for each $t\in(0,T)$, $f\in L^2(\Omega\times(0,T))$, $\mathcal{U}_0\in H^1(\Omega)$, and $\mathcal{W}_0\in L^2(\Omega)$. For the definition of the above boundary spaces, we refer, e.g., to [24], vol. I.

The corresponding variational formulation of problem (1)-(4) reads:
Find $u:(0,T)\to H^1(\Omega)$, such that for $a.e.\ t\in(0,T)$, $u(t)=\Phi(t)$ on Γ_D and

$$\left(\frac{\partial^2 u}{\partial t^2},v\right)+a(u,v)+\sqrt{c_0}\langle\frac{\partial u}{\partial t},v\rangle_{\Gamma_{AB}}=(f,v)+\langle\Psi,v\rangle_{\Gamma_{Ne}}\quad\forall v\in V, \tag{5}$$

with

$$a(u,v)=c_0\int_\Omega \nabla u\cdot\nabla v\,\mathrm{d}\mathbf{x},\ \ (f,v)=\int_\Omega fv\,\mathrm{d}\mathbf{x},\ \ \langle\zeta,v\rangle_{\mathcal{D}}=\int_{\mathcal{D}}\zeta v\,\mathrm{d}s,\ \ \mathcal{D}=\Gamma_{Ne}\text{ or }\mathcal{D}=\Gamma_{AB}, \tag{6}$$

and $V=\{v\in H^1(\Omega):v=0\text{ on }\Gamma_D\}$. We recall that the bilinear form $a(\cdot,\cdot)$ is symmetric, V-elliptic, and continuous. These conditions imply that problem (5) admits a unique solution u satisfying a stability estimate (see, e.g., [24]). For the proof of stability and uniqueness of the continuous acoustic problem in the case of ABCs, we refer to [28] where the similar case of elastodynamics linear problems is analyzed.

3 B-splines and NURBS-based isogeometric analysis

We briefly recall the semidiscrete continuos-in-time numerical approximation of the acoustic wave problem in the strong (1-4) and weak (5) forms that are based on IGA collocation and Galerkin, respectively. Given an open *knot vector*

$$\{\xi_1=0,\ldots,\xi_{v+p+1}=1\}, \tag{7}$$

of non-decreasing real numbers in the reference interval [0, 1], we consider univariate B-spline basis functions N_i^p having support (ξ_i, ξ_{i+p+1}), $i = 1, 2, ..., \nu$, where p is the polynomial degree and ν is the number of basis functions and control points. Starting from piecewise-constant functions corresponding to degree $p = 0$, then B-splines are built recursively (see, e.g., [32]). If internal nodes are not repeated, B-spline basis functions are C^{p-1}-continuous, whereas if the associated knot has multiplicity equal to α, the basis is C^k-continuous, with $k = p - \alpha$. In particular, at that location when a knot has multiplicity $\alpha = p$, the basis is C^0-continuous. In order that all considered functions are at least globally continuous, we assume that the maximum knot multiplicity is p. For the sake of simplicity, we take the case of same degree p in each direction. The case of different degrees can be defined analogously. We denote by $\widehat{\Omega} := (0, 1) \times (0, 1)$ the two-dimensional parametric domain built from a knot vector (7) in each direction, and $\mathbf{C}_{i,j}$ is the net of ν^2 control points, $i, j = 1, ..., \nu$. Similarly, the multi-dimensional B-spline basis functions on $\widehat{\Omega}$ are obtained by tensor product as

$$B_{i,j}^p(\xi, \eta) = N_i^p(\xi) N_j^p(\eta), \ i, j = 1, \ldots, \nu. \tag{8}$$

Finally, given the one-dimensional spline space $\text{span}\{N_i^p(\xi), i = 1, \ldots, \nu\}$, we obtain the bi-variate spline space:

$$\widehat{\mathcal{S}}_h = \text{span}\{B_{i,j}^p(\xi, \eta), \ i, j = 1, \ldots, \nu\}; \tag{9}$$

(see [30] and references therein for details). We introduce a NURBS basis function of degree p as

$$R_i^p(\xi) = \frac{N_i^p(\xi)\omega_i}{w(\xi)}, \tag{10}$$

where $w(\xi) = \sum_{\hat{i}=1}^{\nu} N_{\hat{i}}^p(\xi)\omega_{\hat{i}} \in \widehat{\mathcal{S}}_h$ is a weight function, and we build NURBS basis functions on the two-dimensional parametric space $\widehat{\Omega}$ as

$$R_{i,j}^p(\xi, \eta) = \frac{B_{i,j}^p(\xi, \eta)\omega_{i,j}}{w(\xi, \eta)}. \tag{11}$$

Here, $w(\xi, \eta) = \sum_{\hat{i},\hat{j}=1}^{\nu} B_{\hat{i},\hat{j}}^p(\xi, \eta)\omega_{\hat{i},\hat{j}}$ and $\omega_{i,j} \in \mathbb{R}$ is the two-dimensional weight. See [20] for the precise definition of the weights ω_i and $\omega_{i,j}$. We recall that NURBS basis functions obtained by the span of the basis functions (11) have the same continuity and support of B-splines. If we confine ourselves to the case of a *single-patch* domain Ω as a NURBS region associated with the net $\mathbf{C}_{i,j}$, we can define the geometrical map $\mathbf{F} : \widehat{\Omega} \to \Omega$:

$$\mathbf{F}(\xi, \eta) = \sum_{i,j=1}^{\nu} R_{i,j}^p(\xi, \eta)\mathbf{C}_{i,j}. \tag{12}$$

According to the IGA paradigm, the span of the *push-forward* of the basis functions (11) provides the space of NURBS scalar fields on the domain Ω:

$$\mathcal{N}_h := \text{span}\{R^p_{i,j} \circ \mathbf{F}^{-1},\ i, j = 1, \ldots, \nu\}. \tag{13}$$

3.1 IGA collocation discretization of the acoustic problem

In this section, we briefly review the IGA collocation method (see [1, 3, 31]) and apply it to the acoustic wave problem (1)-(4). We choose as collocation points the classical Greville abscissae

$$\overline{\xi}_i \doteq (\xi_{i+1} + \xi_{i+2} + \ldots + \xi_{i+p})/p,\ i = 1, \ldots, \nu, \tag{14}$$

associated with the given knot vector (7), where $\overline{\xi}_1 = 0$, $\overline{\xi}_\nu = 1$, and the remaining points are in (0, 1) (see [12]). Other choices of isogeometric collocation abscissae have been proposed (see, e.g., [29]). Among these choices, we recall Demko abscissae [13], superconvergent (SC) points [2], Cauchy–Galerkin (CG) points, and alternating/clustered superconvergent (ASC/CSC) points [25]. Demko and Greville points share an $O(h^{p-1})$ convergence order for odd p and $O(h^p)$ for even p. SC and ASC/CSC points improve the convergence order to $O(h^{p+1})$ for odd p, but retain an $O(h^p)$ order for even p. CG points have $O(h^p)$ convergence order for both odd and even degrees p. In this work, we will consider for simplicity the Greville points.

Then, we define the grid of collocation points $\tau_{ij} \in \Omega$ by the tensor product

$$\tau_{ij} = \mathbf{F}(\widehat{\tau}_{ij}),\ \widehat{\tau}_{ij} = (\overline{\xi}_i, \overline{\xi}_j) \in \left(\widehat{\overline{\Omega}}\right),\ i, j = 1, \ldots, \nu.$$

For a more straightforward description of the collocation method, it is convenient to enumerate the grid points $\{\tau_{ij}\}$ using one single index. Thus, each collocation point $\tau_{ij} \in \Omega, i, j = 1, \ldots, \nu$, corresponds to the point P_ℓ of the tensor product grid, $\ell = 1, \ldots, \nu^2$. We also introduce two disjoint sets of indexes $\mathcal{I}_\Omega := \{\ell | P_\ell \in \Omega\}$ and $\mathcal{I}_\Gamma := \{\ell | P_\ell \in \Gamma\}$, associated to internal and boundary points, respectively. In particular, $\mathcal{I}_\Gamma := \mathcal{I}_{\Gamma_D} \cup \mathcal{I}_{\Gamma_{Ne}} \cup \mathcal{I}_{\Gamma_{AB}}$, where $\mathcal{I}_{\Gamma_D} := \{\ell | P_\ell \in \Gamma_D\}$, $\mathcal{I}_{\Gamma_{Ne}} := \{\ell | P_\ell \in \Gamma_{Ne}\}$ and $\mathcal{I}_{\Gamma_{AB}} := \{\ell | P_\ell \in \Gamma_{AB}\}$. We denote by $\mathcal{I} := \mathcal{I}_\Omega \cup \mathcal{I}_\Gamma$ the set of ν^2 indexes of the whole grid of mesh points. Therefore, we obtain the IGA collocation semi-discrete continuous-in-time approximation of the acoustic problem (1)-(4) by imposing the continuous problem (1) at the Greville collocation points as follows:

$$\frac{\partial^2 u}{\partial t^2}(P_\ell, t) - c_0 \Delta u(P_\ell, t) = f(P_\ell, t), \quad \ell \in \mathcal{I}_\Omega,\ t \in (0, T), \tag{15}$$

with initial conditions

$$u(P_\ell, 0) = \mathcal{U}_0(P_\ell), \qquad \frac{\partial u}{\partial t}(P_\ell, 0) = \mathcal{W}_0(P_\ell), \qquad \ell \in \mathcal{I}, \tag{16}$$

and boundary conditions

$$u(P_\ell,t)=\Phi(P_\ell,t),\ \ell\in\mathcal{I}_{\Gamma_D},\qquad \frac{\partial u}{\partial \mathbf{n}}(P_\ell,t)=\Psi(P_\ell,t),\ \ell\in\mathcal{I}_{\Gamma_{Ne}},\ t\in(0,T), \tag{17}$$

$$\frac{1}{\sqrt{c_0}}\frac{\partial u}{\partial t}(P_\ell,t)+\frac{\partial u}{\partial \mathbf{n}}(P_\ell,t)=0,\ \ell\in\mathcal{I}_{\Gamma_{AB}},\ t\in(0,T). \tag{18}$$

The semi-discrete collocation problem (15)-(18) consists of finding a vector $\mathbf{u}=\{u_\ell,\ \ell\in\mathcal{I}\}$, corresponding to elements $\{u_{ij},\ i,j=1,...,\nu\}$ that allow to write the IGA solution as

$$u(\mathbf{x},t)=\sum_{i=1}^{\nu}\sum_{j=1}^{\nu}u_{ij}R_{ij}^{p,q}\circ\mathbf{F}^{-1}(\mathbf{x},t), \tag{19}$$

according to (12) and (13). We introduce now the IGA collocation matrices D_r associated to r-th derivatives at collocation points, for $r=0,\ 1,\ 2$, where D_0, D_1, and D_2 account for the identity, $\frac{\partial}{\partial\mathbf{n}}$, and Δ operators, respectively. Then, equations (15)-(18) can be expressed in matrix form as a system of second-order ordinary differential equations [37]:

$$\frac{\partial^2}{\partial t^2}[D_0\mathbf{u}(t)]_\ell-c_0[D_2\mathbf{u}(t)]_\ell=[\mathbf{f}(t)]_\ell,\ \ell\in\mathcal{I}_\Omega, \tag{20}$$

$$[D_0\mathbf{u}(0)]_\ell=[\mathcal{U}_\mathbf{0}]_\ell,\quad \frac{\partial}{\partial t}[D_0\mathbf{u}(0)]_\ell=[\mathcal{W}_\mathbf{0}]_\ell,\quad \ell\in\mathcal{I}, \tag{21}$$

$$[D_0\mathbf{u}(t)]_\ell=[\Phi(t)]_\ell,\ \ell\in\mathcal{I}_{\Gamma_D},\ [D_1\mathbf{u}(t)]_\ell=[\Psi(t)]_\ell,\ \ell\in\mathcal{I}_{\Gamma_{Ne}}, \tag{22}$$

$$\frac{1}{\sqrt{c_0}}\frac{\partial u}{\partial t}[D_0\mathbf{u}(t)]_\ell+[D_1\mathbf{u}(t)]_\ell=0,\ \ell\in\mathcal{I}_{\Gamma_{AB}} \tag{23}$$

where $[\mathbf{w}]_\ell$ is the ℓ-th element of a general vector $\mathbf{w}$ and $[D_r]_\ell$ is the ℓ-th row of the collocation matrix D_r, $r=0,1,2$. Moreover, $\mathbf{u}(t):=[u(P_\ell,t)]$, $\ell\in\mathcal{I}$, $\mathbf{f}(t):=[f(P_\ell,t)]$, $\ell\in\mathcal{I}$, $\mathcal{U}_\mathbf{0}:=[\mathcal{U}_0(P_\ell)]$, $\ell\in\mathcal{I}$, $\mathcal{W}_\mathbf{0}:=[\mathcal{W}_0(P_\ell)]$, $\ell\in\mathcal{I}$, $\Phi(t):=[\Phi(P_\ell,t)]$, $\ell\in\mathcal{I}_{\Gamma_D}$, $\Psi(t):=[\Psi(P_\ell,t)]$, $\ell\in\mathcal{I}_{\Gamma_{Ne}}$, and all vectors are assigned equal to zero elsewhere.

3.2 IGA Galerkin discretization of the acoustic problem

Starting from the variational form of the acoustic wave problem (5), we replace the L^2-inner products and the bilinear form (6) with their IGA quadrature-based approximations. Then, the semidiscrete continuous-in-time problem reads: for each $t\in(0,T)$, find $u_h\in\mathcal{N}_h$ such that

$$\left(\frac{\partial^2 u_h}{\partial t^2},v\right)_h+a_h(u_h,v)+\sqrt{c_0}\langle\frac{\partial u_h}{\partial t},v\rangle_{h,\Gamma_{AB}}=(f,v)_h+\langle\Psi,v\rangle_{h,\Gamma_{Ne}}\quad\forall v\in\mathcal{N}_h, \tag{24}$$

where $(\cdot,\cdot)_h$, $a_h(\cdot,\cdot)$, $\langle\cdot,\cdot\rangle_{h,\Gamma_{AB}}$, and $\langle\cdot,\cdot\rangle_{h,\Gamma_{Ne}}$ are the IGA L^2- quadrature, stiffness, and boundary bilinear forms, respectively. The algebraic form of (24) is obtained by

expanding discrete functions in terms of isogeometric basis functions, thus yielding a system of second-order ordinary differential equations:

$$\mathcal{M}\ddot{\mathbf{u}}(t) + \mathcal{C}\dot{\mathbf{u}}(t) + \mathcal{A}\mathbf{u}(t) = \mathbf{F}(t) + \Theta(t) + \Xi(t) \doteq \mathbf{Y}(t) \tag{25}$$

with initial conditions $\mathbf{u}(0) = \mathcal{U}_{\mathbf{0}}$, $\dot{\mathbf{u}}(0) = \mathcal{W}_{\mathbf{0}}$ (see [36] for details). In system (25), $\mathcal{M}$ and $\mathcal{A}$ are the mass and stiffness IGA Galerkin matrices associated to $(\cdot,\cdot)_h$ and $a_h(\cdot,\cdot)$, respectively, whereas $\mathcal{C}$ accounts for the boundary term $\sqrt{c_0}\langle\cdot,\cdot\rangle_{h,\Gamma_{AB}}$. We recall that $\mathcal{M}$, $\mathcal{C}$, and $\mathcal{A}$ are symmetric, $\mathcal{M}$ is positive definite, whereas $\mathcal{A}$ is positive semi-definite, and $\mathcal{C}$ is positive semi-definite with most elements equal to zero. Finally, $\forall t \in (0,T)$, $\mathbf{u}(t)$ is the vector of coefficients of u_h in the IGA basis, and $\mathbf{F}(t)$, $\Theta(t)$, and $\Xi(t)$ are known vectors accounting for the contribution of f, Φ, and Ψ, respectively.

3.3 The Newmark IGA collocation and Galerkin schemes

We partition the temporal interval $[0,T]$ into N subintervals $[t_{n-1},t_n]$, with $t_0 = 0$, $t_N = T$, $\Delta t = T/N$, $t_n = n\Delta t$, $n = 1,...,N$, and apply the Newmark method [27] to the numerical semi-discrete continuous-in-time approximation of the acoustic wave IGA collocation problem (20)-(23). We obtain the set of recurrence relations at collocation points:

$$[D_0]_\ell \frac{\mathbf{u}_{n+1} - 2\mathbf{u}_n + \mathbf{u}_{n-1}}{\Delta t^2} - c_0[D_2]_\ell\Big[\beta\mathbf{u}_{n+1} + \Big(\frac{1}{2} - 2\beta + \gamma\Big)\mathbf{u}_n + \Big(\frac{1}{2} + \beta - \gamma\Big)\mathbf{u}_{n-1}\Big] =$$

$$\Big[\beta\mathbf{f}_{n+1} + \Big(\frac{1}{2} - 2\beta + \gamma\Big)\mathbf{f}_n + \Big(\frac{1}{2} + \beta - \gamma\Big)\mathbf{f}_{n-1}\Big]_\ell, \quad \ell \in \mathcal{I}_\Omega \tag{26}$$

$$[D_0]_\ell\mathbf{u}_{n+1} = [\Phi_{n+1}]_\ell, \ \ell \in \mathcal{I}_{\Gamma_D}, \quad [D_1]_\ell\mathbf{u}_{n+1} = [\Psi_{n+1}]_\ell, \quad \ell \in \mathcal{I}_{\Gamma_{Ne}}, \tag{27}$$

$$\frac{1}{\sqrt{c_0}}[D_0]_\ell \frac{\gamma\mathbf{u}_{n+1} + (1-2\gamma)\mathbf{u}_n + (\gamma-1)\mathbf{u}_{n-1}}{\Delta t} + [D_1]_\ell\mathbf{u}_{n+1} = 0, \quad \ell \in \mathcal{I}_{\Gamma_{AB}}. \tag{28}$$

We enforce the average of normal derivatives at any corner point involving ABCs and/or Neumann boundary conditions, whereas Dirichlet conditions override ABCs or Neumann ones.

If we consider now the IGA Galerkin approximation (25), the application of the Newmark scheme gives the recurrence relations:

$$\mathcal{M}\frac{\mathbf{u}_{n+1} - 2\mathbf{u}_n + \mathbf{u}_{n-1}}{\Delta t^2} + \mathcal{C}\frac{\gamma\mathbf{u}_{n+1} + (1-2\gamma)\mathbf{u}_n + (\gamma-1)\mathbf{u}_{n-1}}{\Delta t} +$$

$$\mathcal{A}\Big[\beta\mathbf{u}_{n+1} + \Big(\frac{1}{2} - 2\beta + \gamma\Big)\mathbf{u}_n + \Big(\frac{1}{2} + \beta - \gamma\Big)\mathbf{u}_{n-1}\Big] = \Big[\beta\mathbf{Y}_{n+1} + \Big(\frac{1}{2} - 2\beta + \gamma\Big)\mathbf{Y}_n + \Big(\frac{1}{2} + \beta - \gamma\Big)\mathbf{Y}_{n-1}\Big]. \tag{29}$$

Remark 1 In both collocation and Galerkin versions, the second initial vector $\mathbf{u}_1$ can be computed from the first one $\mathbf{u}_0$ associated to initial condition (2)-left applying a second-order explicit one-step method, e.g., an explicit two-stage Runge-Kutta method, thus

preserving the global accuracy of the numerical scheme with respect to the time step Δt and using (2)-right.♦

In spite of the fact that the theoretical analysis for IGA collocation discretizations of elliptic problems in two and three dimensions is still an open issue, several numerical studied investigate the convergence of the method with respect to the discretization parameters p, h, and k in various fields of application (see, e.g., [1, 23, 25, 31]). In this respect, in our previous works [36]-[38], we presented a detailed numerical study of stability, convergence, computational cost, and spectral properties of the IGA collocation and Galerkin approximation of the acoustic wave equation with ABCs. In the present work, we focus on the spectral properties of matrices arising from implicit Newmark schemes, which yield at each time step the solution of the linear system

$$\mathcal{K}\mathbf{u}_{n+1} = \Upsilon(t_{n+1}, t_n, t_{n-1}), \tag{30}$$

with iteration matrix

$$\mathcal{K} = [D_1]_{\ell\in\mathcal{I}_{Ne}\cup\mathcal{I}_{AB}} + \frac{\gamma}{\Delta t\sqrt{c_0}}[D_0]_{\ell\in\mathcal{I}_{AB}} - c_0\beta[D_2]_{\ell\in\mathcal{I}_\Omega} + \frac{1}{\Delta t^2}[D_0]_{\ell\in\mathcal{I}_\Omega} + [D_0]_{\ell\in\mathcal{I}_D}, \tag{31}$$

in the case of IGA collocation (26)-(28), and

$$\mathcal{K} = \frac{\gamma}{\Delta t}\mathcal{C} + \beta\mathcal{A} + \frac{1}{\Delta t^2}\mathcal{M}, \tag{32}$$

in the case of IGA Galerkin (29), respectively. Furthermore, the right terms $\boldsymbol{\Upsilon}(t_{n+1}, t_n, t_{n-1})$ account for the values of initial data $\mathcal{U}_0$, $\mathcal{W}_0$, and of f, Φ, and Ψ at times t_{n+1}, t_n, t_{n-1}.

Remark 2 By using Taylor expansions, it can be proven that the Newmark method is first-order accurate with respect to Δt if $\gamma \neq \frac{1}{2}$, and it is second-order if $\gamma = \frac{1}{2}$. The schemes (26)-(28) and (29) are considered explicit when $\beta = 0$, even if the matrices D_0 in (26) and $\mathcal{M}$ in (29) are not diagonal. Moreover, they coincide with the *Leap-Frog* method when $\gamma = \frac{1}{2}$, which in particular is explicit and second-order accurate with respect to Δt. Nevertheless, the IGA matrices associated to collocation (26)-(28) and Galerkin (29) approximations become denser for increasing p and k, both for explicit ($\beta = 0$) and implicit ($\beta \neq 0$) case, since the corresponding IGA mass matrices are not diagonal. ♦

4 Condition number estimates: conjectures

In Section 3.3, we showed that each step of either the explicit or the implicit method involves the resolution of a linear system, with iteration matrix $\mathcal{K}$, that may be dense and ill conditioned depending on the choice of the IGA parameters. In addition, the behavior of the spectral properties of IGA collocation and Galerkin matrices is of interest not only for possible investigation of efficient preconditioned iterative solutions of the linear systems arising at each step, but also in order to estimate the maximum

allowable time step Δt for explicit Newmark schemes in order to be stable. Unfortunately, the theoretical analysis of spectral bounds for IGA matrices is still an open issue, since the results on eigenvalues and condition number of the IGA mass and stiffness matrices are almost conjectures. Moreover, the suggested bounds are limited to the IGA Galerkin method for the approximation of the Poisson equation with Dirichlet boundary conditions. With regard to this, we recall some condition number estimates that are reported in [16] in the two-dimensional case for the Galerkin isogeometric mass ($\mathcal{M}$) and stiffness ($\mathcal{A}$) matrices. Regardless of the k-regularity of the spline basis functions, the following bounds are shown:

$$cond(\mathcal{M}) \leq cp^2 4^{2p}, \text{ with } c \text{ independent of } h \text{ and } p, \quad cond(\mathcal{A}) \leq c(h)p^8 4^{2p}. \tag{33}$$

In addition, some bounds on the extreme eigenvalues are proven in [16] in the one-dimensional case and in [17] also for the case of dimension $d > 1$. Furthermore, a methodical numerical study has been carried out in [19] in order to investigate the conditioning of Galerkin isogeometric mass and stiffness matrices in d dimensions, yielding the following more detailed estimates:

$$\text{for } k = 0 \text{ regularity:} \quad cond(\mathcal{M}) \approx p^{-d/2} 4^{pd}, \tag{34}$$

$$\text{for } k = p - 1 \text{ regularity:} \quad cond(\mathcal{M}) \approx e^{pd} \quad \text{if } h \leq 1/p \tag{35}$$

$$\text{for } k = 0 \text{ regularity:} \quad cond(\mathcal{A}) \approx \begin{cases} h^{-2}p^2 & \text{if } h \leq (p^{2+d/2}d^{-dp})^{1/2} \\ p^{-d/2}4^{pd} & \text{otherwise,} \end{cases} \tag{36}$$

$$\text{for } k = p - 1 \text{ regularity:} \quad cond(\mathcal{A}) \approx \begin{cases} h^{-2}p \text{ if } h \leq e^{-dp/2} \\ pe^{pd} \quad \text{if } e^{-dp/2} \leq h \leq 1/p. \end{cases} \tag{37}$$

We propose here some additional conjectures that we assume to apply for the extreme eigenvalues and condition number of the mass $\mathcal{M}$ and iteration matrices $\mathcal{K}$ arising from either the IGA collocation (26)-(28) or Galerkin (29) approximations of the acoustic wave equation with Dirichlet and absorbing boundary conditions. In Table 1, we summarize the conjectured estimates for the case of 2-dimensional and 3-dimensional domains, for which we provide an experimental analysis in Section 5, for the $2D$ standard reference square and quarter-of-ring domains, and for the $3D$ standard reference cube and quarter-of-annulus domains. For the sake of simplicity, in Table 1 and in all figures of Section 5, the symbol $\mathsf{cond}(\mathcal{M})$ denotes also the condition number of the collocation mass matrix, which in the previous discussion of Section 3 is denoted by $[D_0]$.

Remark 3 These conjectures stem from numerical simulations performed with $\Delta t = 0.1$. Although this choice of the time step may be not fine enough for real-interest applications and to ensure numerical stability, the tabulated estimates show the behavior of $\mathsf{cond}(\mathcal{K})$ and its extreme eigenvalues when the mass matrix is not predominant over the stiffness matrix. The opposite situation arises when Δt becomes increasingly small, and correspondingly, the coefficient of the mass matrix becomes increasingly

Table 1 Conjectured trends of the extreme eigenvalues $\min|\lambda(\mathcal{K})|$ and $\max|\lambda(\mathcal{K})|$ and of the condition number $\mathsf{cond}(\mathcal{M})$ and $\mathsf{cond}(\mathcal{K})$ of the IGA collocation (26)-(28) and Galerkin (29) problems

	Collocation			Galerkin		
	$2D$ $k=1$	$2D$ $k=p-1$	$3D$ $k=p-1$	$2D$ $k=1$	$2D$ $k=p-1$	$3D$ $k=p-1$
$\mathsf{cond}(\mathcal{M})\approx$	$p^{-1}4^{\frac{3}{2}p}$	e^{p}	$e^{\frac{3}{2}p}$	$p^{-1}4^{2p}$	e^{2p}	e^{3p}
$\min\lvert\lambda(\mathcal{K})\rvert\approx$	$p^{3}4^{-p}$	$p^{3}e^{-p}$	$p^{3}e^{-\frac{3}{2}p}$	$h^{2}p4^{-2p}$	$h^{2}e^{-2p}$	$h^{2}p^{-1}e^{-3p}$
$\max\lvert\lambda(\mathcal{K})\rvert\approx$	$h^{-2}p^{2}$	$h^{-2}p^{2}$	$h^{-2}p^{2}$	$O(1)$	p	$O(1)$
$\mathsf{cond}(\mathcal{K})\approx$	$h^{-2}p^{-1}4^{p}$	$h^{-2}p^{-1}e^{p}$	$h^{-2}p^{-1}e^{\frac{3}{2}p}$	$h^{-2}p^{-1}4^{2p}$	$h^{-2}pe^{2p}$	$h^{-2}pe^{3p}$

large, resulting in the limiting case with iteration matrix $\mathcal{K}$ that approaches the mass matrix $\mathcal{M}$, up to a multiplicative coefficient equal to $1/\Delta t^2$. Therefore, the condition number and extreme eigenvalues of the iteration matrix would tend to show the same trends as for the mass matrix.

5 Numerical results

In [39], we have conducted a systematic numerical study of the eigenvalue distribution, condition number, and sparsity of the mass and iteration matrices arising from the IGA collocation approximation in space and Newmark advancing schemes in time, both explicit and implicit, for the acoustic wave equation in the reference square domain with Dirichlet, Neumann, and absorbing boundary conditions. We report now the results of a more comprehensive numerical study and comparison of the IGA collocation method introduced in Section 3.1, and the IGA Galerkin method introduced in Section 3.2, with reference to the behavior of extreme eigenvalues and condition number of the mass matrix $\mathcal{M}$ and iteration matrix $\mathcal{K}$, varying the degree p, regularity k, and mesh size h. We consider the acoustic wave problem in the reference square domain $\Omega = [0, 1] \times [0, 1]$ and in the quarter of circular ring domain with external and internal radius of 2 and 1, respectively. An example of the latter computational domain is given in Fig. 12d, for the test with piecewise-constant velocity c_0. The case

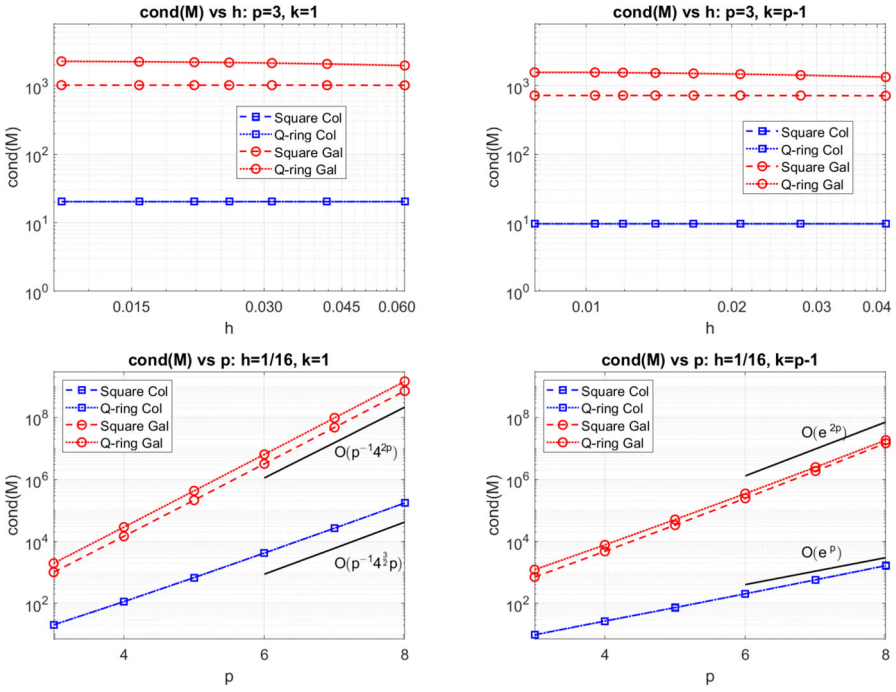

Fig. 1 2D: condition number cond($\mathcal{M}$) of the mass matrix. Left: $k = 1$; right $k = p - 1$. Top: vs h, fixed $p = 3$; bottom: vs p, fixed $h = 1/16$. Dashed (resp. dotted) lines refer to square (resp. quarter-of-ring) domain. The □ (resp. ∘) symbols refer to IGA collocation (resp. Galerkin)

of heterogeneous acoustic wave propagation velocity c_0 in (4) is also considered. In all tests, unless otherwise specified, we fix the time discretization parameters of the Newmark scheme $\Delta t = 0.1$, $\beta = 0.5$, and $\gamma = 0.5$, corresponding to a second-order accurate implicit scheme. All tests have been carried out with MATLAB R2024b using the GeoPDEs 3.0 library (see, e.g., [11, 34]). In particular, the collocation matrices introduced in Section 3.1 are built using the structure `sp_eval`, whereas the condition number is computed as the ratio $(max|\lambda|)/(min|\lambda|)$ between extreme eigenvalues of a given matrix.

2D: condition number of the mass matrix In Fig. 1, we report the condition number $\mathsf{cond}(\mathcal{M})$ of the IGA collocation (□ symbols) and Galerkin (○ symbols) mass matrices for the acoustic wave problem, vs h, for $p = 3$ (top), and vs p, for $h = 1/16$ (bottom), for minimum regularity $k = 1$ (left) and maximum regularity $k = p-1$ (right). Dashed lines refer to square domain, whereas dotted lines refer to quarter-of-ring domain. The numerical results show that if p is fixed (top), the condition number $\mathsf{cond}(\mathcal{M})$ is almost independent of h, in agreement with estimates (34)-(35). For the p-refinement with fixed h (bottom), the condition number $\mathsf{cond}(\mathcal{M})$ of the IGA Galerkin mass matrix grows as $p^{-1}4^{2p}$ in the case of minimal regularity $k = 1$, whereas for maximal regularity $k = p - 1$, the growth is e^{2p}. In the case of IGA collocation, the numerical results are better, since the condition number $\mathsf{cond}(\mathcal{M})$ grows as $p^{-1}4^{\frac{3}{2}p}$ in the case of minimal regularity $k = 1$ and e^p for maximal regularity $k = p - 1$.

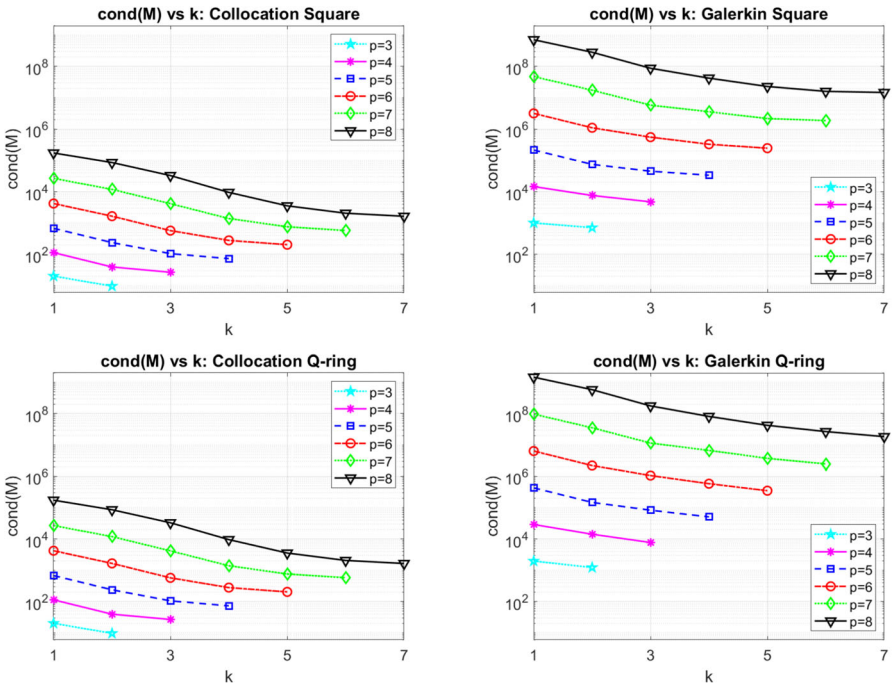

Fig. 2 2D: condition number $\mathsf{cond}(\mathcal{M})$ of the mass matrix vs k, for $p = 3, \ldots, 8$, fixed $h = 1/16$. Left: IGA collocation; right: IGA Galerkin. Top: square domain; bottom: quarter-of-ring domain

In Fig. 2, we report the condition number $\mathsf{cond}(\mathcal{M})$ for increasing k and six values of polynomial degree p, fixed $h = 1/16$. The left (resp. right) panels refer to IGA collocation (resp. IGA Galerkin) approximation; the top (resp. bottom) panels refer to square (resp. quarter-of-ring) domain. It seems that $\mathsf{cond}(\mathcal{M})$ decreases exponentially when the regularity k increases.

We observe that all above considerations are valid regardless of the shape of the domain, either square or quarter-of-ring, and in addition, the values of $\mathsf{cond}(\mathcal{M})$ for the IGA Galerkin case are always higher than for the collocation case.

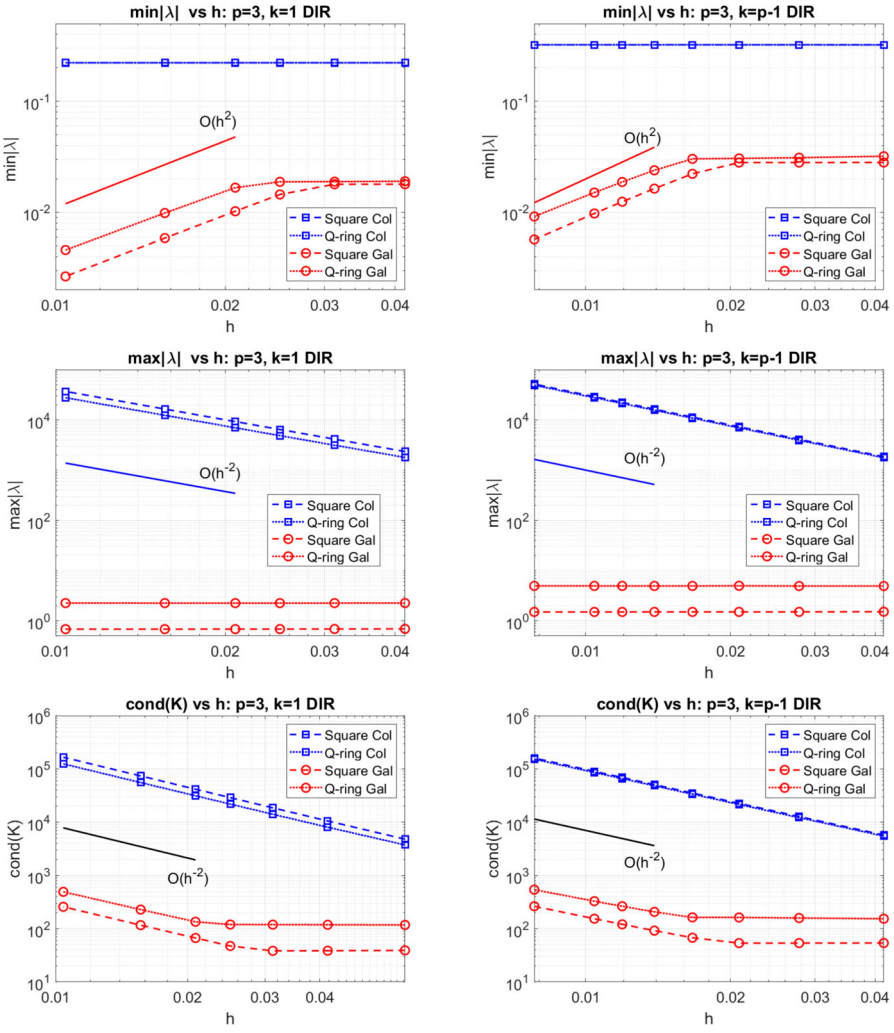

Fig. 3 2D: extreme eigenvalues and condition number of the iteration matrix vs h, fixed $p = 3$, for the acoustic wave problem with Dirichlet boundary conditions. Left: $k = 1$; right $k = p - 1$. Top: $\min|\lambda(\mathcal{K})|$; central: $\max|\lambda(\mathcal{K})|$; bottom: $\mathsf{cond}(\mathcal{K})$. Dashed (resp. dotted) lines refer to square (resp. quarter of ring) domain. The $\square$ (resp. $\circ$) symbols refer to IGA collocation (resp. Galerkin)

2D: extreme eigenvalues and condition number of the iteration matrix with Dirichlet boundary conditions In Fig. 3 (resp. Figure 4), we report the extreme eigenvalues $\min|\lambda(\mathcal{K})|$ (top), $\max|\lambda(\mathcal{K})|$ (central), and the condition number $\mathsf{cond}(\mathcal{K})$ (bottom) of the IGA collocation (□ symbols) and Galerkin (○ symbols) iteration matrices for the acoustic wave problem with Dirichlet boundary conditions, vs h, fixed $p = 3$ (resp. $p = 5$), for minimum regularity $k = 1$ (left) and maximum regularity $k = p - 1$ (right). Dashed lines refer to square domain, whereas dotted lines refer to quarter-of-ring domain.

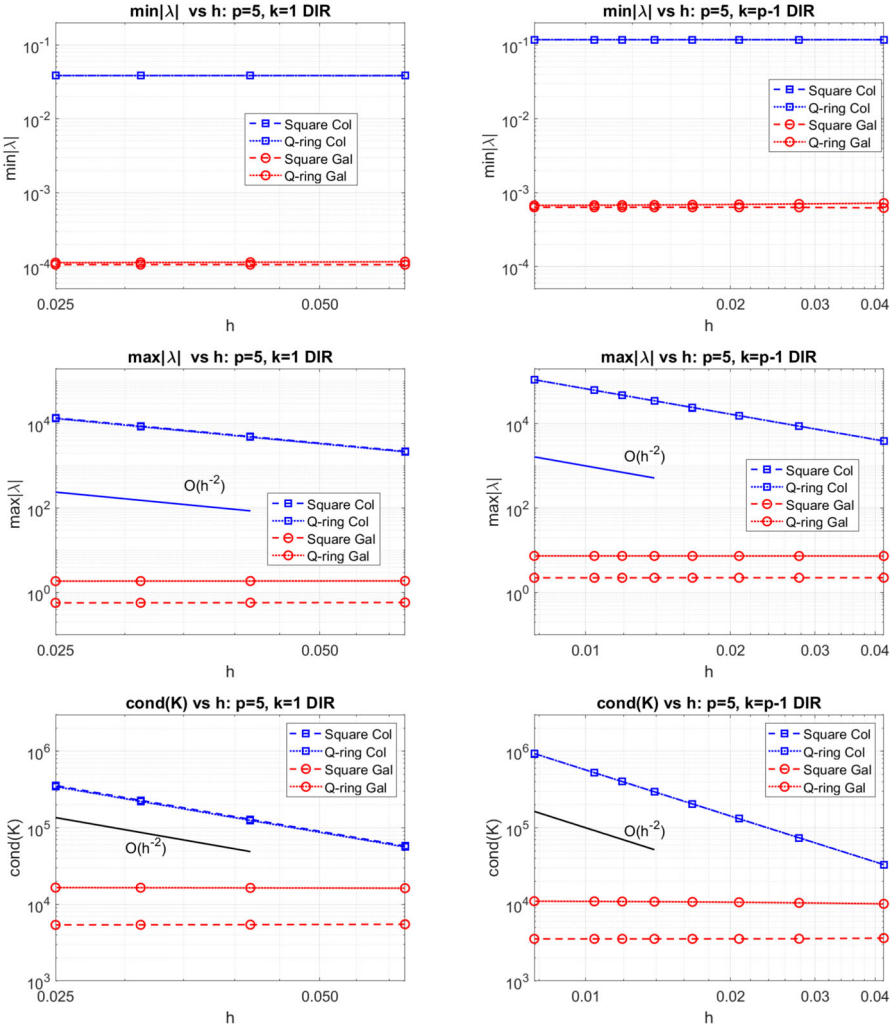

Fig. 4 2D: extreme eigenvalues and condition number of the iteration matrix vs h, fixed $p = 5$, for the acoustic wave problem with Dirichlet boundary conditions. Left: $k = 1$; right $k = p - 1$. Top: $\min|\lambda(\mathcal{K})|$; central: $\max|\lambda(\mathcal{K})|$; bottom: $\mathsf{cond}(\mathcal{K})$. Dashed (resp. dotted) lines refer to square (resp. quarter of ring) domain. The □ (resp. ○) symbols refer to IGA collocation (resp. Galerkin)

For the choice of the degree $p = 3$, it seems that

1) $\min|\lambda(\mathcal{K})|$: is independent of h for IGA collocation; behaves as h^2 for IGA Galerkin, if h is suitably small, whereas it is almost independent of h when h increases;
2) $\max|\lambda(\mathcal{K})|$: behaves as h^{-2} for IGA collocation; it is independent of h for IGA Galerkin;

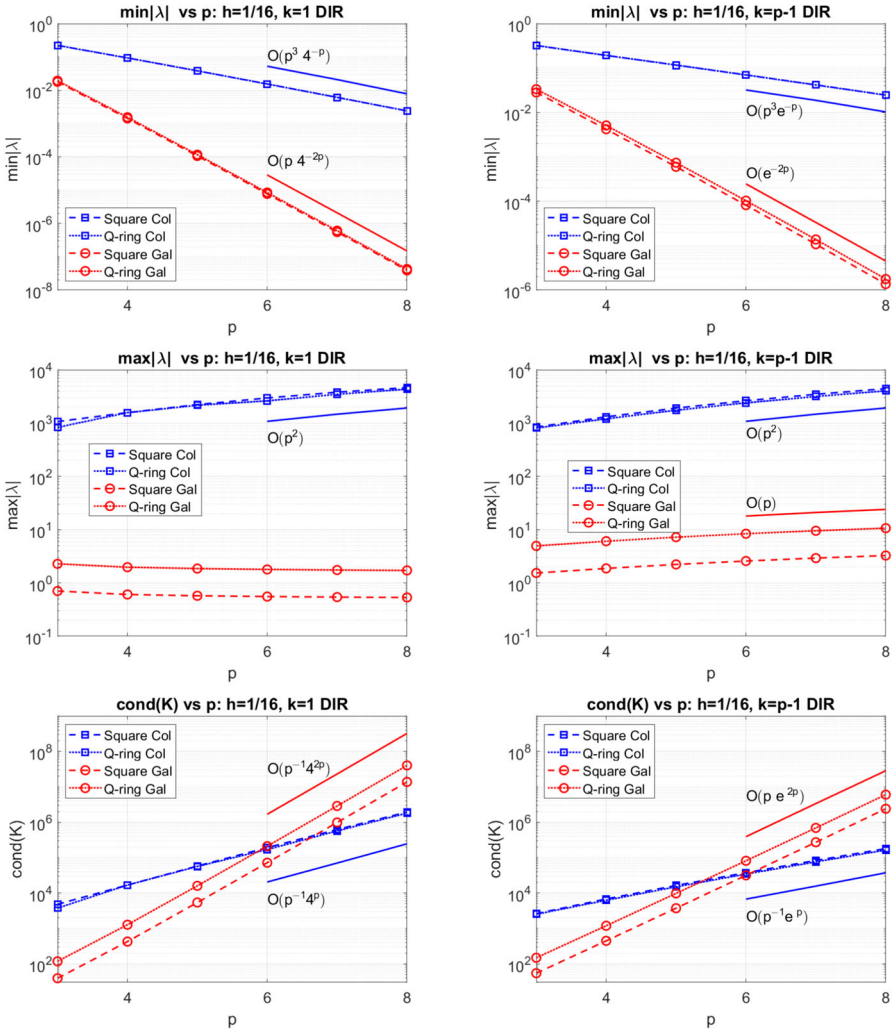

Fig. 5 2D: extreme eigenvalues and condition number of the iteration matrix vs p, fixed $h = 1/16$, for the acoustic wave problem with Dirichlet boundary conditions. Left: $k = 1$; right $k = p - 1$. Top: $\min|\lambda(\mathcal{K})|$; central: $\max|\lambda(\mathcal{K})|$; bottom: $\mathsf{cond}(\mathcal{K})$. Dashed (resp. dotted) lines refer to square (resp. quarter of ring) domain. The $\square$ (resp. $\circ$) symbols refer to IGA collocation (resp. Galerkin)

3) The condition number $\mathsf{cond}(\mathcal{K})$: behaves as h^{-2} for IGA collocation; behaves as h^{-2} for IGA Galerkin, if h is suitably small, whereas it is almost independent of h when h increases.

If we consider instead the values obtained for $p = 5$, we clearly observe the same trends in the case of IGA collocation. On the other hand, in the case of IGA Galerkin, the extreme eigenvalues and condition number seem to be independent of h, even for small values of h. The reason for this trends can be mainly attributed to the fact that min $|\lambda(\mathcal{K})|$ (resp. $\mathsf{cond}(\mathcal{K})$) decreases (resp. increases) much more rapidly with increasing p in the IGA Galerkin case in comparison to what occurs in the collocation

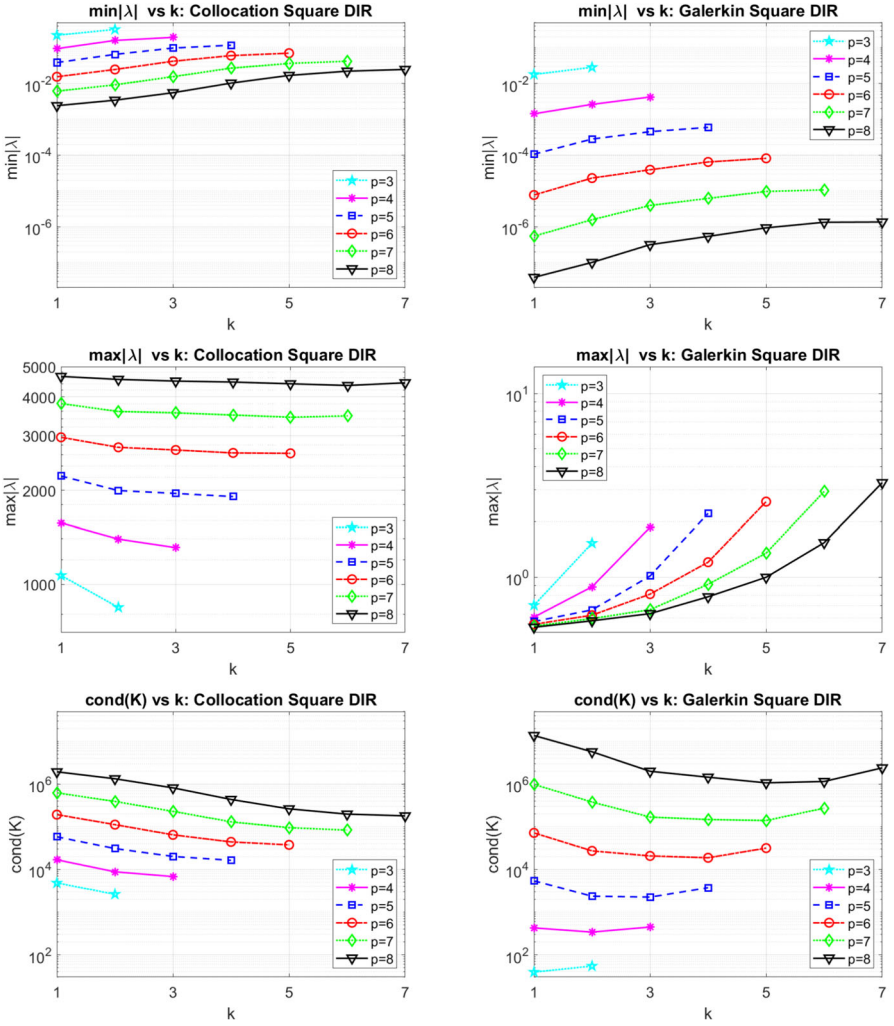

Fig. 6 2D: extreme eigenvalues and condition number of the iteration matrix vs k, for $p = 3, \ldots, 8$, fixed $h = 1/16$, for the acoustic wave problem with Dirichlet boundary conditions and square domain. Left: IGA collocation; right IGA Galerkin. Top: min $|\lambda(\mathcal{K})|$; central: max $|\lambda(\mathcal{K})|$; bottom: $\mathsf{cond}(\mathcal{K})$

case (see Fig. 5), making the reduction of h practically negligible with respect to the variation of extreme eigenvalues and condition number.

In all cases, the gap between collocation and Galerkin lines slightly reduces when moving from $p = 3$ to $p = 5$ plots.

In Fig. 5, we report the same data as in Fig. 3, varying degree p, fixed $h = 1/16$. The numerical results show that

1) In the case of minimal regularity $k = 1$, $\min |\lambda(\mathcal{K})|$ seems to decrease as $p^3 4^{-p}$ for IGA collocation and as $p4^{-2p}$ for IGA Galerkin, whereas in the case of maximal

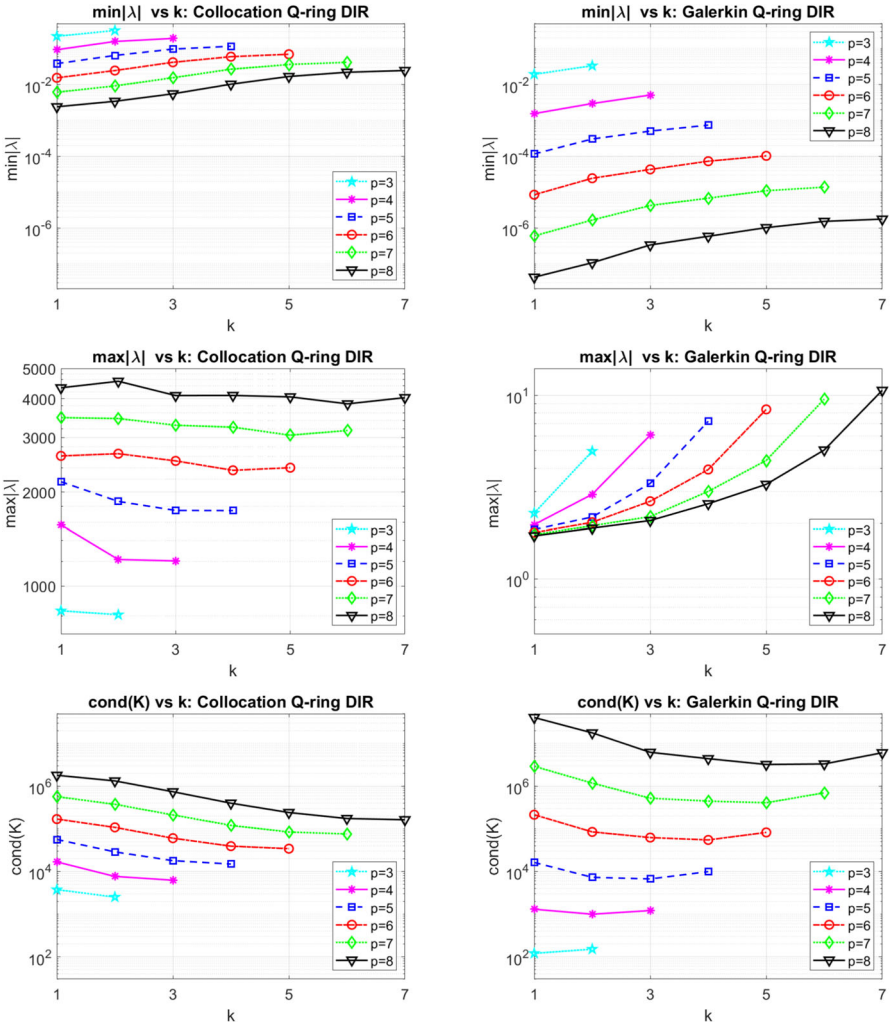

Fig. 7 2D: extreme eigenvalues and condition number of the iteration matrix vs k, for $p = 3, ..., 8$, fixed $h = 1/16$, for the acoustic wave problem with Dirichlet boundary conditions and quarter-of-ring domain. Left: IGA collocation; right IGA Galerkin. Top: $\min |\lambda(\mathcal{K})|$; central: $\max |\lambda(\mathcal{K})|$; bottom: $\mathsf{cond}(\mathcal{K})$

regularity $k = p - 1$, $\min |\lambda(\mathcal{K})|$ seems to decrease as $p^3 e^{-p}$ for IGA collocation and as e^{-2p} for IGA Galerkin;

2) In the case of minimal regularity $k = 1$, $\max |\lambda(\mathcal{K})|$ seems to grow as p^2 for IGA collocation and to be independent of p for IGA Galerkin, whereas in the case of maximal regularity $k = p-1$, $\max |\lambda(\mathcal{K})|$ seems to grow as p^2 for IGA collocation and as p for IGA Galerkin;
3) In the case of minimal regularity $k = 1$, $\mathsf{cond}(\mathcal{K})$ seems to grow as $p^{-1}4^p$ for IGA collocation and as $p^{-1}4^{2p}$ for IGA Galerkin, whereas in the case of maximal regularity $k = p - 1$, $\mathsf{cond}(\mathcal{K})$ seems to grow as $p^{-1}e^p$ for IGA collocation and as pe^{2p} for IGA Galerkin.

Similarly to what we have observed for the IGA mass matrices, the numerical results are better in the case of IGA collocation iteration matrices, if we compare the slope of the lines, i.e., the exponential behavior 4^{2p} and e^{2p} for IGA Galerkin, with respect to 4^p and e^p for IGA collocation, improving again estimates (36)-(37). On the other hand, the condition number is lower in the case of IGA Galerkin for small values of degree p, whereas it is lower in the case of IGA collocation for large values of p, regardless of the geometry and of regularity k.

In Figs. 6 and 7, we report the extreme eigenvalues $\min |\lambda(\mathcal{K})|$ (top), $\max |\lambda(\mathcal{K})|$ (central), and the condition number $\mathsf{cond}(\mathcal{K})$ (bottom) of the IGA collocation (left) and Galerkin (right) iteration matrices, for the acoustic wave problem with Dirichlet boundary conditions, for increasing k and four values of polynomial degree p, fixed $h = 1/16$. Figures 6 and 7 refer to the square and quarter-of-ring domain, respectively.

It seems that, regardless of the shape of the domain,

1) $\min |\lambda(\mathcal{K})|$ increases both for IGA collocation and IGA Galerkin;
2) $\max |\lambda(\mathcal{K})|$ is roughly independent of k, with some slight oscillations in the case of quarter-of-ring domain for IGA collocation, whereas it increases exponentially when the regularity k increases for IGA Galerkin;
3) $\mathsf{cond}(\mathcal{K})$ decreases when k increases for IGA collocation, whereas for IGA Galerkin, it decreases exponentially when the regularity k increases, but it increases when the regularity k is close to the maximum value $p - 1$.

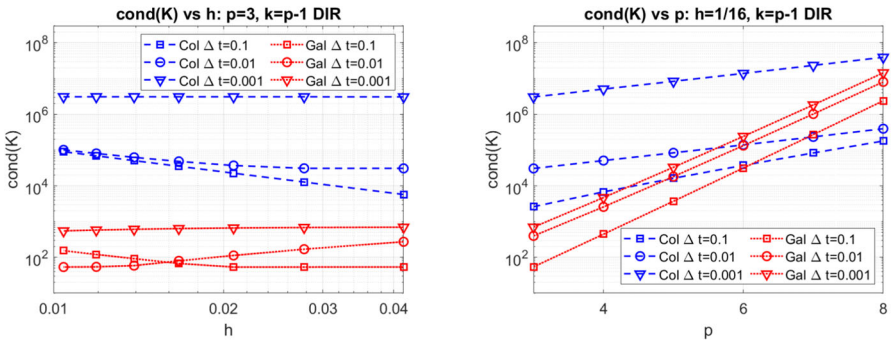

Fig. 8 2D: condition number $\mathsf{cond}(\mathcal{K})$ of the iteration matrix varying Δt. Left: vs h, fixed $p = 3$; right vs p, fixed $h = 1/16$. The blue dashed (resp. red dotted) lines refer to IGA collocation (resp. Galerkin)

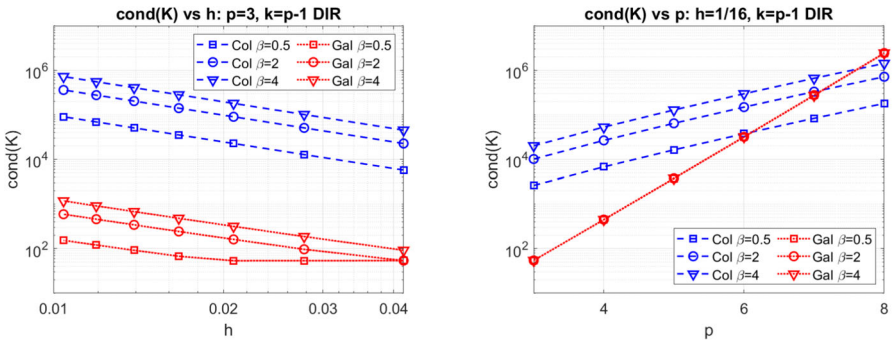

Fig. 9 2D: condition number $\mathsf{cond}(\mathcal{K})$ of the iteration matrix varying β. Left: vs h, fixed $p = 3$; right vs p, fixed $h = 1/16$. The blue dashed (resp. red dotted) lines refer to IGA collocation (resp. Galerkin)

2D: condition number of the iteration matrix varying Δt In Fig. 8, we report condition number $cond(\mathcal{K})$ of the IGA collocation and Galerkin iteration matrices in the case of the reference square domain, for three different values of time step Δt, as a function of mesh size h, fixed degree $p = 3$ (left), and as a function of degree p, fixed mesh size $h = 1/16$ (right), and maximal regularity $k = p - 1$ in both cases. Let us recall that for decreasing values of Δt, the mass matrices D_0 and $\mathcal{M}$ get more predominant over the Laplacian matrices D_2 and $\mathcal{A}$, due to the multiplicative coefficient $1/\Delta t^2$ in Newmark formulas (26) and (29), and consequently, the iteration matrix basically tends to approach the mass matrix scaled by the coefficient $1/\Delta t^2$, which becomes increasingly large. Therefore, if we consider smaller values of Δt, for h approaching zero, the condition number of the iteration matrix tends to become constant, as is the case of the mass matrix (see Fig. 1), leading to a flat line for the smaller value of Δt. On the other hand, for increasing p, no changes in the trends are observed since the trends for both the mass and iteration matrices show the same dependence on the degree p (see Figs. 3 and 5, bottom panels).

2D: condition number of the iteration matrix varying β In Fig. 9, we report condition number $cond(\mathcal{K})$ of the IGA collocation and Galerkin iteration matrices in the case of the reference square domain, for three different values of the Newmark parameter β, as a function of mesh size h, fixed degree $p = 3$ (left), and as a function of degree p, fixed mesh size $h = 1/16$ (right), and maximal regularity $k = p - 1$ in both cases. We note that the asymptotic behavior of $cond(\mathcal{K})$ with respect to h and p remains unchanged with the only difference that lines are shifted upward when β increases in almost all cases.

2D: condition number of the iteration matrix with absorbing boundary conditions In Fig. 10, for the sake of brevity, we simply report the condition number $\mathsf{cond}(\mathcal{K})$ of the IGA collocation and Galerkin iteration matrices for the acoustic wave problem with absorbing boundary conditions (4), vs h, for $p = 3$ (top), and vs p, for $h = 1/16$ (bottom), using the same setting as in Figs. 1, 3, and 5.

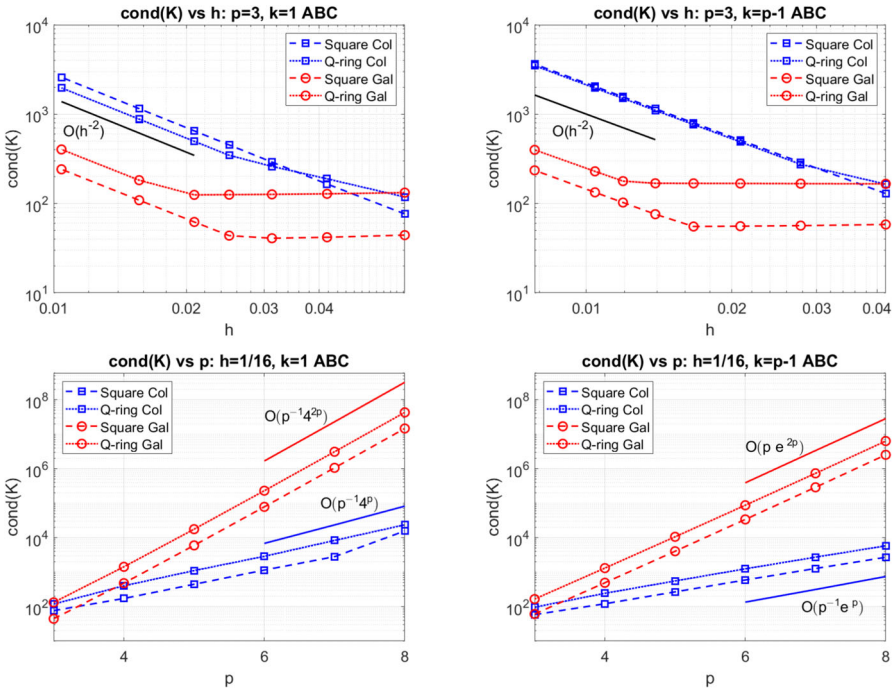

Fig. 10 2D: condition number $\mathsf{cond}(\mathcal{K})$ of the iteration matrix. Left: $k = 1$; right $k = p - 1$. Top: vs h, fixed $p = 3$; bottom: vs p, fixed $h = 1/16$. Dashed (resp. dotted) lines refer to square (resp. quarter of ring) domain. The □ (resp. ∘) symbols refer to IGA collocation (resp. Galerkin)

The numerical results show the same trends as for the case of Dirichlet boundary conditions shown in Figs. 3 and 5.

In Fig. 11, we report the condition number $\mathsf{cond}(\mathcal{K})$ for increasing k and six values of polynomial degree p, fixed $h = 1/16$, and the same setting of plots as in Fig. 2. It seems that $\mathsf{cond}(\mathcal{K})$ decreases exponentially when the regularity k increases, but it increases when the regularity k is close to the maximum value $p - 1$, and this behavior is observed either for IGA collocation or Galerkin. As before, we also note that all above considerations are valid regardless of the shape of the domain, and in addition, the values of $\mathsf{cond}(\mathcal{K})$ for the IGA Galerkin case are always higher than for the collocation case.

2D: condition number of the iteration matrix varying c_0 We now consider the case of heterogeneous acoustic wave propagation velocity c_0 in (1) with absorbing boundary conditions (4). In this test, the coefficient c_0 is no longer constant but is given either by

(c.1) The smooth function $c_0(x_1, x_2) = \exp(-s(x_1 + x_2))$, $s \in [-2, 2]$ (see Fig. 12, for square (a) and quarter-of-ring (b) domains);

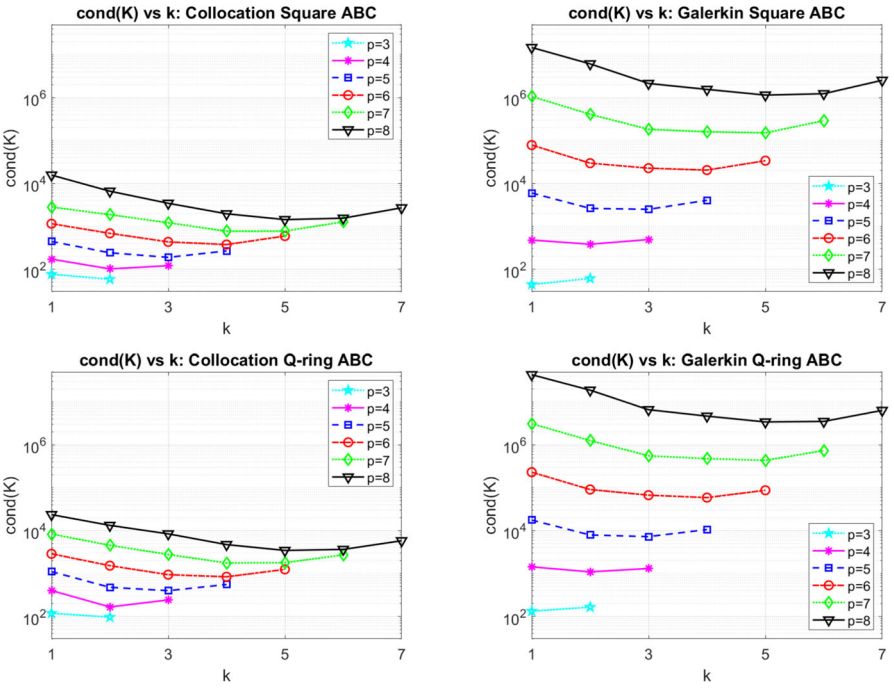

Fig. 11 2D: condition number $\mathsf{cond}(\mathcal{K})$ of the iteration matrix vs k, $p = 3, ..., 8$, for the acoustic wave problem with absorbing boundary conditions. Left: IGA collocation; right: IGA Galerkin. Top: square domain; bottom: quarter-of-ring domain

(c.2) A piecewise-constant function $c_0 = 10^s$, with $s \in [-4, 4]$ in the central (yellow) portion of the domain and $c_0 = 1$ in the external (blue) portion of the domain (see Fig. 12c, d).

In Table 2, we report condition number $cond(\mathcal{K})$ of the IGA Galerkin (left) and collocation (right) iteration matrices, respectively, for acoustic wave propagation velocity given as in (c.1), for the reference square (1^{st} and 3^{rd} columns) and quarter-of-ring domains (2^{nd} and 4^{th} columns), as a function of parameter s, varying s in $[-2, 2]$, fixed degree $p = 4$, maximal regularity $k = 3$, mesh size $h = 1/16$. These results

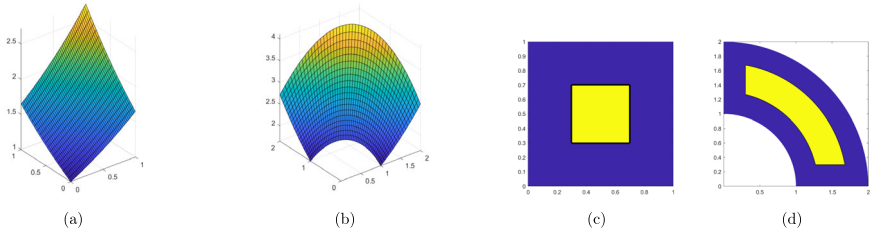

Fig. 12 Plot of velocity $c_0(x_1, x_2) = exp(-s(x_1 + x_2))$ on square (**a**) and quarter-of-ring (**b**) domain; piecewise-constant function on square (**c**) and quarter-of-ring (**d**) domain

Table 2 2D: heterogeneous acoustic wave propagation velocity c_0 (c.1): condition number $\mathsf{cond}(\mathcal{K})$ of the iteration matrix vs $c_0(x_1, x_2) = \exp(-s(x_1 + x_2))$, varying $s \in [-2, 2]$, fixed $p = 4, k = 3, h = 1/16$

s	Galerkin square	Q-ring	Collocation square	Q-ring
-2.0	7.456e+03	2.100e+04	5.266e+03	2.436e+04
-1.0	1.632e+03	4.837e+03	7.764e+02	1.470e+03
0.0	4.907e+02	1.308e+03	1.208e+02	2.424e+02
1.0	1.631e+03	1.308e+03	2.305e+02	1.123e+02
2.0	4.865e+03	2.833e+03	3.537e+02	7.265e+01

Galerkin (left) and collocation (right). 1st and 3rd columns: square domain; 2nd and 4th columns: quarter-of- ring domain

show that in almost all cases, the condition number generally becomes as larger as the parameter s in the test function $c_0(x_1, x_2) = \exp(-s(x_1 + x_2))$ moves farther from the value 0.0 (corresponding to a constant velocity c_0), with the exception of the results in the case of collocation and quarter-of-ring domain, since the condition number continues to decrease slightly when s grows from the value 0.0 to the value 2.0. Finally, in Table 3, we report the same data with the same setting as in Table 2, for an abrupt discontinuity of propagation velocity given as in (c.2). Again, we observe the same behavior as in the case of (c.1), since the condition number increases more and more when the parameter s, that is chosen to compute $c_0 = 10^s$ in the central portion of the domain, moves away from the value $c_0 = 1$, corresponding to the choice $s = 0$, that is the value of the piecewise-constant function in the portion of the domain towards the external boundary.

3D numerical tests We finally report some preliminary results for two different 3D domains: the reference cube $[0, 1]^3$ and the quarter of annulus with outer radius 2, inner radius 1, and height 1. We consider the IGA collocation and Galerkin approximation of the acoustic wave problem with Dirichlet boundary conditions and constant acoustic wave propagation velocity $c_0 = 1$. In Fig. 13, we report the condition number of the mass matrices D_0 and $\mathcal{M}$ (top-left) and of iteration matrix $\mathcal{K}$ (top-right), and of extreme eigenvalues of the iteration matrix $\max|\lambda(\mathcal{K})|$ (bottom-left) and $\min|\lambda(\mathcal{K})|$ (bottom-right), varying the degree p simultaneously in the three directions, and fixing mesh size $h = 1/16$, time step $\Delta t = 0.1$, and Newmark parameters $\beta = 0.5$ and

Table 3 2D: heterogeneous acoustic wave propagation velocity c_0 (c.2): condition number $\mathsf{cond}(\mathcal{K})$ of the iteration matrix vs $c_0 = 10^s$, varying $s \in [-4, 4]$ in the central portion of the domain and $c_0 = 1$ in the external portion of the domain (see Fig. 12c, d), fixed $p = 4$, $k = 3$, $1/h = 1/16$

s	Galerkin square	Q-ring	Collocation square	Q-ring
-4	2.108e+03	5.516e+03	2.295e+02	2.424e+02
-2	1.893e+03	5.082e+03	1.899e+02	2.424e+02
0	4.907e+02	1.308e+03	1.208e+02	2.424e+02
2	8.033e+03	1.527e+04	2.268e+03	4.876e+03
4	7.178e+05	1.297e+06	2.266e+05	4.871e+05

Galerkin (left) and collocation (right). 1st and 3rd columns: square domain; 2nd and 4th columns: quarter-of- ring domain

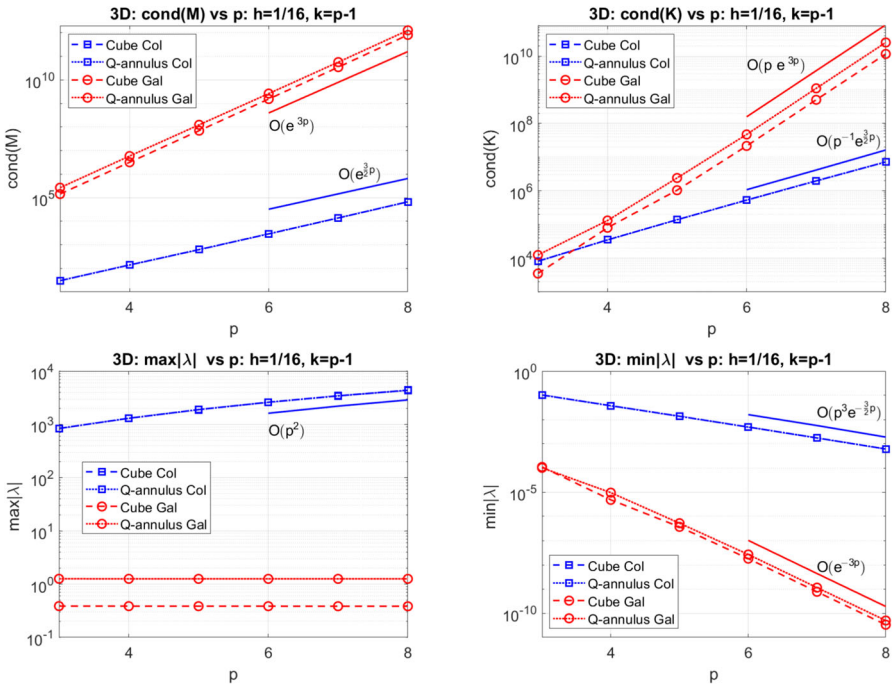

Fig. 13 3D test: condition number $\mathsf{cond}(\mathcal{M})$ of the mass matrix (top-left) and $\mathsf{cond}(\mathcal{K})$ of the iteration matrix (top-right), extreme eigenvalues of the iteration matrix $\max|\lambda(\mathcal{K})|$ (bottom-left) and $\min|\lambda(\mathcal{K})|$ (bottom-right) vs p, with maximum regularity $k = p - 1$, fixed $h = 1/16$, $\Delta t = 0.1$, $\beta = 0.5$, for the acoustic wave problem with Dirichlet boundary conditions

$\gamma = 0.5$. For the sake of brevity, we consider the classical isogeometric case with maximum regularity $k = p - 1$ only. In all tests, the curves show the same qualitative behavior in p as in the 2D case (see Fig. 1, bottom-right panel, Fig. 5, right panels, Fig. 10, bottom-right), up to the dimension d of the domain, namely, the asymptotic behaviors e^p and e^{2p}, which seems to hold in the 2D case, become $e^{\frac{3}{2}p}$ and e^{3p}, respectively, in the 3D case. To summarize, the numerical results show that

1) In the case of IGA collocation, $\mathsf{cond}(D_0)$ seems to grow as $e^{\frac{3}{2}p}$, whereas in the case of IGA Galerkin, $\mathsf{cond}(\mathcal{M})$ seems to grow as e^{3p};
2) $\mathsf{cond}(\mathcal{K})$ seems to grow as $p^{-1}e^{\frac{3}{2}p}$ for IGA collocation and as pe^{3p} for IGA Galerkin;
3) $\max|\lambda(\mathcal{K})|$ seems to grow as p^2 for IGA-collocation, and it seems to be constant for IGA Galerkin;
4) $\min|\lambda(\mathcal{K})|$ seems to decrease as $p^3e^{-\frac{3}{2}p}$ for IGA collocation and as e^{-3p} for IGA Galerkin.

These numerical results show that the condition number $\mathsf{cond}(\mathcal{K})$ is better in the case of IGA collocation iteration matrices than in the case of IGA Galerkin, except

for the choice of minimum degree $p = 3$, in which case they are approximately equal. For the sake of clarity, we point out that we have not performed 3D tests varying the mesh size h, as we did in Figs. 1 (top), 3, 4, and 10 (top) for the 2D case, but we can reasonably hypothesize that the behavior of condition number and extreme eigenvalues with respect to h in 3D is similar to that in 2D, as we have also conjectured in Table 1.

6 Conclusions

In this paper, we have studied experimentally the spectral properties of the mass and iteration matrices related to the IGA collocation and Galerkin approximation of the acoustic wave equation with standard Dirichlet or first-order absorbing boundary conditions, while the time-advancing scheme is based on the Newmark method.

We have presented a direct and detailed numerical comparison between the collocation and Galerkin IGA methods with regard to extreme eigenvalues and condition number of their mass and iteration matrices, varying the polynomial degree p, mesh size h, regularity k, and the type of boundary conditions that can be either Dirichlet or absorbing. We have also generalized and improved some conjectures that are available in the literature only for matrices resulting from IGA Galerkin approximation of the Poisson problem for the case of Dirichlet boundary conditions, through a systematic comparison with the collocation case. Our results show that similar bounds hold for the condition number of mass and iteration matrices for the two IGA discretizations of acoustic wave problems, and in most cases, the collocation bounds are better than the Galerkin ones. We have also considered the case of heterogeneous acoustic wave propagation velocity in the computational domain, given either by a smooth function or by a piecewise-constant function.

These results can be of interest not only in the field of acoustic wave equations for stability analysis of explicit Newmark schemes in order to estimate the maximum allowable time step Δt, but also for several partial differential equations that trace back to the Laplacian operator. Furthermore, they can be considered as an important starting point for developing efficient preconditioning methods for the iteration matrices, both in the case of explicit and implicit time-advancing schemes. Future extensions of the present study could include also more advanced boundary conditions with high-order derivatives in space and time, as well as perfectly matched layer (PML) boundary conditions. The generalization to elastic wave equations is also of relevant interest.

Acknowledgements The author would like to thank the anonymous reviewers for their helpful and insightful comments and suggestions, which helped to improve the quality of this manuscript.

Author Contributions The author confirms being the sole contributor of this work.

Funding Open access funding provided by Università degli Studi di Milano within the CRUI-CARE Agreement. This work was supported by grants of MIUR (PRIN 202232A8AN_003 and PRIN P2022B38NR_002), funded by European Union - Next Generation EU.

Declarations

Conflict of interest The author declares no competing interests.

References

1. Auricchio, F., Beirão da Veiga, L., Hughes, T.J.R., Reali, A., Sangalli, G.: Isogeometric collocation methods. Math. Mod. Meth. Appl. Sci. **20**(11), 2075–2107 (2010)
2. Anitescu, C., Yue, J., Zhang, Y.J., Rabczuk, T.: An isogeometric collocation method using superconvergent points. Comput. Methods Appl. Mech. Engrg. **284**, 1073–1097 (2015)
3. Auricchio, F., Beirão da Veiga, L., Hughes, T.J.R., Reali, A., Sangalli, G.: Isogeometric collocation for elastostatics and explicit dynamics. Comput. Meth. Appl. Mech. Eng. **249–252**, 2–14 (2012)
4. Bayliss, A., Gunzburger, M., Turkel, E.: Boundary conditions for the numerical solution of elliptic equations in exterior regions. SIAM J. Appl. Math. **42**(2), 430–451 (1982)
5. Bayliss, A., Turkel, E.: Radiation boundary conditions for wave-like equations. Comm. On Pure App. Math. **33**(6), 707–725 (1980)
6. Bazilevs, Y., Beirão da Veiga, L., Cottrell, J.A., Hughes, T.J.R., Sangalli, G.: Isogeometric analysis: approximation, stability and error estimates for *h*-refined meshes. Math. Mod. Meth. Appl. Sci. **16**, 1–60 (2006)
7. Beirão da Veiga, L., Buffa, A., Sangalli, G., Vázquez, R.: Mathematical analysis of variational isogeometric methods. Acta Numer **23**, 157–287 (2014)
8. Clayton, R., Engquist, B.: Absorbing boundary conditions for acoustic and elastic wave equations. Bull. Seism. Soc. Am. **67**(6), 1529–1540 (1977)
9. Cottrell, J.A., Hughes, T.J.R., Bazilevs, Y.: Isogeometric analysis. Wiley, Towards integration of CAD and FEA (2009)
10. Cottrell, J., Reali, A., Bazilevs, Y., Hughes, T.J.R.: Isogeometric analysis of structural vibrations. Comput. Methods Appl. Mech. Engrg. **195**, 5257–5296 (2006)
11. De Falco, C., Reali, A., Vázquez, R.: GeoPDEs: a research tool for isogeometric analysis of PDEs. Adv. Eng. Softw. **42**(12), 1020–1034 (2011)
12. de Boor, C.: phA practical guide to splines. Springer (2001)
13. Demko, S.: On the existence of interpolation projectors onto spline spaces. J. of Approx. Theory **43**, 151–156 (1985)
14. Engquist, B., Majda, A.: Radiation boundary conditions for acoustic and elastic wave equations. Commun. Pure Appl. Math. **32**, 313–357 (1979)
15. Evans, J.A., Hiemstra, R.R., Hughes, T.J.R., Reali, A.: Explicit higher-order accurate isogeometric collocation methods for structural dynamics. Comput. Methods Appl. Mech. Engrg. **338**(15), 208–240 (2018)
16. Gahalaut, K., Tomar, S.: Condition number estimates for matrices arising in the isogeometric discretization. Tech. Report 2012-23, RICAM (2012)
17. Garoni, C., Manni, C., Pelosi, F., Serra Capizzano, S., Speelers, H.: On the spectrum of stiffness matrices arising from isogeometric analysis. Numer. Math. **127**(4), 751–799 (2014)
18. Givoli, D.: Non-reflecting boundary conditions. J. Comput. Phys. **94**(1), 1–29 (1991)
19. Gervasio, P., Dedé, L., Chanon, O., Quarteroni, A.: A computational comparison between isogeometric analysis and spectral element methods: accuracy and spectral properties. J. Sci. Comp. **83**, 1–45 (2020)

20. Hughes, T.J.R., Cottrell, J.A., Bazilevs, Y.: Isogeometric analysis: CAD, finite elements, NURBS, exact geometry, and mesh refinement. Comp. Meth. Appl. Mech. Engrg. **194**, 4135–4195 (2005)
21. Hughes, T.J.R., Reali, A., Sangalli, G.: Isogeometric methods in structural dynamics and wave propagation. *In COMPDYN 2009*, M. Papadrakakis et al. (eds.), (2009)
22. Junger, M.C., Feit, D.: Sound. Structures and their Interaction. MIT Press, Cambridge, MA (1986)
23. Kruse, R., Nguyen-Thanh, N., De Lorenzis, L., Hughes, T.J.R.: Isogeometric collocation for large deformation elasticity and frictional contact problems. Comp. Meth. Appl. Mech. Engrg. **296**, 73–112 (2015)
24. Lions, J.L., Magenes, E.: Nonhomogeneous Boundary Value Problems and Applications, vol. 1. Springer, Berlin, Heidelberg, New York (1972)
25. Montardini, M., Sangalli, G., Tamellini, L.: Optimal-order isogeometric collocation at Galerkin superconvergent points. Comput. Methods Appl. Mech. Engrg. **316**, 741–757 (2017)
26. Mur, G.: Absorbing boundary conditions for the finite-difference approximation of the time-domain electromagnetic-field equations. IEEE Trans. Elect. Compat. **23**(4), 377–382 (1981)
27. Newmark, N. M.: A method of computation for structural dynamics. Proc. ASCE J. Eng. Mech. (EM3) **85**, 67–94 (1959)
28. Quarteroni, A., Tagliani, A., Zampieri, E.: Generalized Galerkin approximations of elastic waves with absorbing boundary conditions. Comput. Methods Appl. Mech. Engrg. **163**, 323–341 (1998)
29. Ren, J., Lin, H.: A survey on isogeometric collocation methods with applications. Mathematics **11**(469), 323–341 (2023)
30. Rogers, D.F.: *An Introduction to NURBS With Historical Perspective*. Academic Press, (2001)
31. Schillinger, D., Evans, J.A., Reali, A., Scott, M.A., Hughes, T.J.R.: Isogeometric collocation: cost comparison with Galerkin methods and extension to adaptive hierarchical NURBS discretizations. Comp. Meth. Appl. Mech. Engrg. **267**, 170–232 (2013)
32. Schumaker, L.L.: Spline Functions: Basic Theory, 3rd edn. Cambridge University Press, Cambridge, Cambridge Mathematical Library (2007)
33. S. V. Tsynkov Numerical solution of problems on unbounded domains. A review . Appl. Numer. Math. **27**, 465-532 (1998)
34. R. Vázquez. A new design for the implementation of isogeometric analysis in Octave and Matlab: GeoPDEs 3.0. IMATI REPORT Series 16-02 (2016)
35. Venås, J.V., Kvamsdal, T.: Isogeometric analysis of acoustic scattering with perfectly matched layers (IGAPML). Comput. Methods Appl. Mech. Engrg. **401**, 115647 (2022)
36. Zampieri, E., Pavarino, L.F.: Explicit second order isogeometric discretizations for acoustic wave problems. Comput. Methods Appl. Mech. Engrg. **348**, 776–795 (2019)
37. Zampieri, E., Pavarino, L.F.: Isogeometric collocation discretizations for acoustic wave problems. Comput. Methods Appl. Mech. Engrg. **385**, 114047 (2021)
38. Zampieri, E., Pavarino. L. F.: A numerical comparison of Galerkin and collocation isogeometric approximations of acoustic wave problems. Appl. Numer. Math. https://doi.org/10.1016/j.apnum.2023.06.001 (2023)
39. Zampieri, E., Pavarino, L. F.: Conditioning and spectral properties of isogeometric collocation matrices for acoustic wave problems. Adv. Comp. Math. **50**, 16 (2024). https://doi.org/10.1007/s10444-024-10113-y
40. Zampieri, E., Scacchi, S., Pavarino, L.F.: Overlapping Schwarz preconditioners for isogeometric discretizations of acoustic wave problems. Comput. Methods Appl. Mech. Engrg. **448**, 118397 (2026)